Research Article | Vol. 26, No. 3 | 5 Feb 2018 | OPTICS EXPRESS 2400
Optics EXPRESS

Assessing performance of modern Brillouin spectrometers

ZACHARY COKER,[1,*] MARIA TROYANOVA-WOOD,[1] ANDREW J. TRAVERSO,[1] TALGAT YAKUPOV,[2] ZHANDOS N. UTEGULOV,[2,3] AND VLADISLAV V. YAKOVLEV[1]

[1]*Texas A&M University, College Station, Texas 77843, USA*
[2]*Optics Laboratory, Center of Energy and Advanced Material Science, National Laboratory of Astana, Nazarbayev University, Astana 010000, Kazakhstan*
[3]*Department of Physics, School of Science and Technology, Nazarbayev University, Astana 010000, Kazakhstan*
ZacharyCoker@physics.tamu.edu

Abstract: Brillouin spectroscopy and imaging has experienced a renaissance in recent years seeing vast improvements in methodology and increasing number of applications. With this resurgence has come the development of new spontaneous Brillouin instruments that often tout superior performance compared to established conventional systems such as tandem Fabry-Perot interferometers (TFPI). The performance of these new systems cannot always be thoroughly examined beyond the scope of the intended application, as applications often take precedence in reports. We therefore present evaluation of three modern Brillouin spectrometers: two VIPA-based spectrometers with wavelength-specific notch filters, and one scanning 6-pass TFPI. Performance analysis is presented along with a discussion about the dependence of measurements on excitation laser source and the various susceptibilities of each system.

OCIS codes: (290.5830) Scattering, Brillouin; (300.6190) Spectrometers.

References and links

1. G. Antonacci, M. R. Foreman, C. Paterson, and P. Török, "Spectral broadening in Brillouin imaging," Appl. Phys. Lett. **103**(22), 5–8 (2013).
2. Z. Meng, A. J. Traverso, and V. V. Yakovlev, "Background clean-up in Brillouin microspectroscopy of scattering medium," Opt. Express **22**(5), 5410–5415 (2014).
3. G. Scarcelli and S. H. Yun, "Multistage VIPA etalons for high-extinction parallel Brillouin spectroscopy," Opt. Express **19**(11), 10913–10922 (2011).
4. K. Berghaus, J. Zhang, S. H. Yun, and G. Scarcelli, "High-finesse sub-GHz-resolution spectrometer employing VIPA etalons of different dispersion," Opt. Lett. **40**(19), 4436–4439 (2015).
5. G. Antonacci, G. Lepert, C. Paterson, and P. Török, "Elastic suppression in Brillouin imaging by destructive interference," Appl. Phys. Lett. **107**(6), 61102 (2015).
6. K. Elsayad, S. Werner, M. Gallemí, J. Kong, E. R. Sánchez Guajardo, L. Zhang, Y. Jaillais, T. Greb, and Y. Belkhadir, "Mapping the subcellular mechanical properties of live cells in tissues with fluorescence emission-Brillouin imaging," Sci. Signal. **9**(435), rs5 (2016).
7. M. Vaughan, *The Fabry-Perot Interferometer: History, Theory, Practice and Applications* (CRC Press, 1989).
8. Z. Meng, A. J. Traverso, C. W. Ballmann, M. A. Troyanova-Wood, and V. V. Yakovlev, "Seeing cells in a new light: a renaissance of Brillouin spectroscopy," Adv. Opt. Photonics **8**(2), 300–327 (2016).
9. K. J. Koski and J. L. Yarger, "Brillouin imaging," Appl. Phys. Lett. **87**(6), 20–23 (2005).
10. Z. Meng and V. V. Yakovlev, "Precise determination of Brillouin scattering spectrum using a virtually imaged phase array (VIPA) spectrometer and charge-coupled device (CCD) camera," Appl. Spectrosc. **70**(8), 1356–1363 (2016).
11. C. Song, E. Sánchez-Ortiga, M. R. Foreman, and P. Török, "Optimisation of a single stage VIPA spectrometers (Conference Presentation)," Proc. SPIE **10067**, 100670N (2017).
12. Z. N. Utegulov, J. M. Shaw, B. T. Draine, S. A. Kim, and W. L. Johnson, "Surface-plasmon enhancement of Brillouin light scattering from gold-nanodisk arrays on glass," in M. I. Stockman, ed. (2007), p. 66411M.
13. W. L. Johnson, S. A. Kim, Z. N. Utegulov, J. M. Shaw, and B. T. Draine, "Optimization of arrays of gold nanodisks for plasmon-mediated brillouin light scattering," J. Phys. Chem. C **113**(33), 14651–14657 (2009).
14. G. Scarcelli, W. J. Polacheck, H. T. Nia, K. Patel, A. J. Grodzinsky, R. D. Kamm, and S. H. Yun, "Noncontact three-dimensional mapping of intracellular hydromechanical properties by Brillouin microscopy," Nat. Methods **12**(12), 1132–1134 (2015).
15. Z. Steelman, Z. Meng, A. J. Traverso, and V. V. Yakovlev, "Brillouin spectroscopy as a new method of

#313638 https://doi.org/10.1364/OE.26.002400
Journal © 2018 Received 16 Nov 2017; revised 18 Jan 2018; accepted 19 Jan 2018; published 23 Jan 2018

Optics EXPRESS

screening for increased CSF total protein during bacterial meningitis," J. Biophotonics **8**(5), 408–414 (2015).
16. M. Troyanova-Wood, C. Gobbell, Z. Meng, A. A. Gashev, and V. V. Yakovlev, "Optical assessment of changes in mechanical and chemical properties of adipose tissue in diet-induced obese rats," J. Biophotonics **10**(12), 1694–1702 (2017).
17. I. Remer and A. Bilenca, "Background-free Brillouin spectroscopy in scattering media at 780 nm via stimulated Brillouin scattering," Opt. Lett. **41**(5), 926–929 (2016).
18. A. J. Traverso, J. V. Thompson, Z. A. Steelman, Z. Meng, M. O. Scully, and V. V. Yakovlev, "Dual Raman-Brillouin microscope for chemical and mechanical characterization and imaging," Anal. Chem. **87**(15), 7519–7523 (2015).
19. F. Scarponi, S. Mattana, S. Corezzi, S. Caponi, L. Comez, P. Sassi, A. Morresi, M. Paolantoni, L. Urbanelli, C. Emiliani, L. Roscini, L. Corte, G. Cardinali, F. Palombo, J. R. Sandercock, and D. Fioretto, "High-performance versatile setup for simultaneous Brillouin-Raman microspectroscopy," Phys. Rev. X **7**(3), 031015 (2017).
20. J. R. Sandercock, "Brillouin scattering study of SbSI using a double-passed, stabilised scanning interferometer," Opt. Commun. **2**(2), 73–76 (1970).
21. A. J. Martin and W. Brenig, "Model for Brillouin scattering in amorphous solids," Phys. Status Solidi **64**(1), 163–172 (1974).
22. M. Shirasaki, A. N. Akhter, and C. Lin, "Virtually imaged phased array with graded reflectivity," IEEE Photonics Technol. Lett. **11**(11), 1443–1445 (1999).
23. S. Xiao, A. M. Weiner, and C. Lin, "A dispersion law for virtually imaged phased-array spectral dispersers based on paraxial wave theory," IEEE J. Quantum Electron. **40**(4), 420–426 (2004).
24. G. Scarcelli and S. H. Yun, "Confocal Brillouin microscopy for three-dimensional mechanical imaging," Nat. Photonics **2**(1), 39–43 (2007).
25. K. Berghaus, S. H. Yun, and G. Scarcelli, "High speed sub-GHz spectrometer for Brillouin scattering analysis," J. Vis. Exp. **106**, 53468 (2016).
26. M. J. Weber, *Handbook of Optical Materials*, 10th ed. (CRC press, 2003).
27. J. Rheims, J. Köser, and T. Wriedt, "Refractive-index measurements in the near-IR using an Abbe refractometer," Meas. Sci. Technol. **8**(6), 601–605 (1999).
28. G. W. Willard, "Ultrasonic absorption and velocity measurements in numerous liquids," J. Acoust. Soc. Am. **12**(3), 438–448 (1941).
29. K. Liang, J. Xu, P. Zhang, Y. Wang, Q. Niu, L. Peng, and B. Zhou, "Temperature dependence of the Rayleigh Brillouin spectrum linewidth in air and nitrogen," Sensors (Basel) **17**(7), 1503 (2017).
30. A. Fiore, J. Zhang, P. Shao, S. H. Yun, and G. Scarcelli, "High-extinction VIPA-based Brillouin spectroscopy of turbid biological media," Appl. Phys. Lett. **108**, 1–9 (2016).

1. Introduction

Many new approaches have been proposed for improving Brillouin spectrometer designs from implementing different collection geometries, to notch filters, to sequential VIPAs [1–6]. The history and advancements of Brillouin spectroscopy have been covered extensively [7–9], and a large number of reports are available on improvements for system optimization and spectral analysis [10,11]. Likewise, reports covering the broad range of Brillouin applications in materials and nano-science [12,13], biomedical imaging [14–17], and multi-modal Brillouin systems [18,19] are readily available.

In this report, we present a performance evaluation of three Brillouin spectrometers across a range of acquisition times. The spectrometers evaluated were a conventional scanning 6-pass tandem Fabry-Perot interferometer (TFPI) system with single photon counter, and two custom-built spectrometers using virtual imaged phase array (VIPA) dispersion optics and atomic absorption-based notch filters.

The purpose of this investigation was to provide a detailed look at the performance of two types of modern Brillouin spectrometers. Additionally, we present information critical to understanding how each spectrometer design (either static, dispersive VIPA-based design, or conventional commercially-available scanning TFPI) impacts performance and applicability to a wide range of potential investigations. Furthermore, in characterizing our spectrometers, we set out to answer three fundamental questions: "*How accurate can our systems be? How long does it take for each system to achieve this level of accuracy? – Can we do better?*" By answering these questions, we not only evaluate our systems performance, but also develop a better understanding of how to further improve modern Brillouin spectrometer designs.

To evaluate our spectrometers and their performance, we have examined the accuracy and spectral resolution of Brillouin measurements acquired from acetone (a reliable, commonly-used calibration sample) against a range of spectra acquisitions times. The result of each

Optics EXPRESS

system analysis is presented alongside the others to allow the reader to easily examine the performances and differences between each system and design.

Ultimately, the two most important goals for modern Brillouin spectrometers is to offer sub-GHz spectral resolution and to achieve high accuracy in both Brillouin shift (peak position) and Brillouin linewidth (FWHM) measurements. The sub-GHz resolution provides high spectral contrast between elastic-scattered Rayleigh signal, and the inelastic-scattered Brillouin signal, while high accuracy of Brillouin shift and linewidth measurements provides accurate measurements of material's elastic modulus and viscoelastic properties. There is a strong focus on improving spectral contrast with the development of VIPA-based spectrometers.

Every new technique and design falls into one of only two established methods for high accuracy Brillouin measurements: scanning methods using scanning interferometers, and static or non-scanning angular dispersive etalon methods. Each new proposed design claims an advantage over others, but few researchers have presented how their system performance varies with time. Most Brillouin spectroscopy reports focus primarily on specific instrument application and use, often only providing data acquired under optimal conditions or very specific sample material. Such specific data might not be applicable across different fields or when studying different materials. Without a clear understanding of how the different types of modern spectrometers perform across a variety of acquisition times under the same conditions, researchers cannot make an informed decision about which spectrometer design best suits their needs.

2. Methods, materials, and analysis

The performance of three Brillouin spectrometers were analyzed in this investigation: a scanning 6-pass TFPI with a single photon counter shown in Fig. 1 (right) and two custom-built VIPA-based spectrometers shown in Fig. 1 (left). The demonstrated VIPA design shows the 780 nm system; the 532 nm setup has 1064 nm laser and I_2 filter instead of ^{85}Rb, but is otherwise identical. The theory and development of each of these systems has been covered in great detail previously [7,8,18,20–25], therefore only a brief description of each spectrometer cataloging the most important properties is provided in this report.

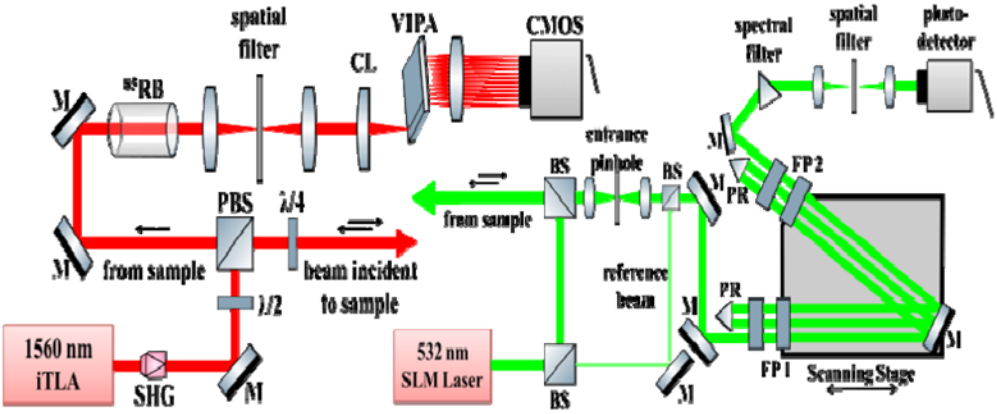

Fig. 1. Schematic diagram of VIPA-based Brillouin spectrometer (left - red) and a scanning 6-pass TFPI-based micro-Brillouin spectrometer (right - green). Abbreviations: (P)BS – (polarizing) beamsplitter; L – lens, ^{85}RB – single-isotope rubidium-filled cell; CL – cylindrical lens, PR – prism, FP – Fabry-Perot cavity, M – mirror.

2.1 Tandem 6-pass Fabry-Perot interferometer

The scanning 6-pass TFPI is equipped with a single photon counter and 1024-channel multichannel analyzer. This system was used to collect two separate data sets in this investigation. Different scanning parameters and laser sources demonstrate measurement

Optics EXPRESS

sensitivity dependence on laser stability and dispersion optics finesse, or free spectral range (FSR). The first data set was acquired using a single longitudinal mode (SLM) laser with 532 nm wavelength (Torus 532, Laser Quantum). We set the total scan amplitude to 93.92 GHz, i.e. approximately twice that of the interferometer's tuned FSR of 50 GHz, effectively scanning ± 49.96 GHz from incidence. The inter-channel frequency resolution, determined by the scan amplitude divided by the total number of channels, was 91.7 MHz. For the second data set, the excitation source was another SLM laser of wavelength 532 nm (Verdi G2, Coherent Inc) and we tuned TFPI for a total scan amplitude of 16.57 GHz and FSR of 8.285 GHz. The inter-channel frequency resolution for the second data set was then 16.18 MHz. We used a 10x 0.25 NA microscope objective to focus the incident light, and to collect the Brillouin back-scattered light from the sample. Examples of each raw spectra and Lorentz fits from the TFPI and VIPA-based spectrometers are provided in Fig. 2.

2.2 VIPA-based spectrometer with 780 nm wavelength

The first of the two VIPA-based Brillouin spectrometers was designed around an excitation source centered at 780.24 nm, with a single isotope ^{85}Rb absorption cell (Opthos Instruments, Inc.) acting as a narrow-band notch filter, a 10x 0.25 NA objective, and VIPA with FSR of 20.43 GHz. The VIPA had an anti-reflection coating optimal for the 780 nm wavelength and net finesse of approximately 40 (with roughly 200 round-trip passes to 1% intensity). The theoretical bandwidth at the output of the VIPA, based on the incident beam parameters and VIPA design was 0.45 GHz (Light Machinery, Inc.). A spherical lens focused the Brillouin spectra output from the VIPA onto a CMOS camera (Neo 5.5 sCMOS; Andor Technology, Inc.). Like the TFPI, two 780 nm laser sources were used to investigate the importance of laser stability on spectral resolution and overall sensitivity and accuracy of measurements.

The first excitation source was an extended cavity diode laser (ECDL) centered at 780.24 nm with output power of ~100 mW (Sacher Lasertechnik; Lion series). An electronic feedback loop and locking device controlled the piezoelectric transducer and thus the output wavelength of the laser. The second source was based on an integrable tunable laser assembly (iTLA) (PurePhotonics; PPCL300) tuned to a central wavelength of 1560.48nm and a MgO-doped PPLN second harmonic generation (SHG) crystal (MSHG1550-1.0-20; Covesion, Ltd) to generate an output wavelength of 780.24 nm with output power up to ~100 mW. The SHG technologies and a fiber amplifier provided a very stable narrow-band, tunable excitation source, greatly simplifying the system.

2.3 VIPA-based spectrometer with 532 nm wavelength

The second VIPA-based Brillouin spectrometers was designed around a single-frequency laser (NKT Photonics.; Koheras BOOSTIK Y10) with 1064 nm center wavelength and 2 W maximum output power. We used a SHG crystal (MSGH1064-1.0-20; Covesion, Ltd.) to generate an output wavelength of 532 nm with output power up to ~150 mW. Similar to the ^{85}Rb absorption cell employed with the 780 nm spectrometer, an I_2 absorption cell (Opthos Instruments, Inc.) was used as the notch filter for the 532 nm VIPA-based spectrometer. The VIPA had an anti-reflection coating optimal for visible light wavelengths, and had FSR of 33.3 GHz, net finesse of 34.6 (with roughly 200 round trips to 1% intensity), and theoretical linewidth and spectral resolution of 0.96 GHz at VIPA output (Light Machinery, Inc.). Brillouin spectra were projected from the VIPA through a spherical lens onto a CCD camera (Newton 971; Andor Technology, Inc.). We note that the overall linewidth of the measured spectra is determined by three primary factors: the material's intrinsic linewidth for Brillouin shift, dispersion relation and finesse of the VIPA, and spectral broadening/distortion effects caused by optical components (objective numerical aperture (NA), lenses, filters, etc.). The 532 nm VIPA-based system used a higher NA objective and VIPA with differing finesse than that of the 780 nm system, and thus we expect larger linewidth measurements. We used a 20x 0.4 NA microscope objective for this spectrometer, as opposed to the 10x 0.25NA objective used for the 780 nm spectrometer. The laser power at the sample for this spectrometer was set to ~0.8 mW, a significantly lower power than the other spectrometers. This power level was

Optics EXPRESS

chosen to avoid detector saturation at long acquisition times (greater than 10 s). While this incident laser power was acceptable for the longer acquisition times, it provided for poor resolution and low signal-noise ratio (SNR) at short acquisition times (less than 0.5 s). This power level was maintained for all spectra acquisition time to maintain uniformity throughout the experiment. Further discussion is provided in the Results section.

2.4 Sample selection and preparation

Acetone was selected as the sample material for this investigation. The Brillouin shifts and viscoelastic properties of acetone are well known (speed of sound, viscosity, refractive index) [26]. Acetone has been used as a test sample in previous experiments [2] and is often used as a reliable calibration sample, and thus is optimal for characterizing the performance of these three spectrometers. Bulk samples were prepared in 20mL glass vials to avoid unwanted backscattered reflections from material boundaries, and all acetone samples were kept at room temperature with their respective spectrometer to ensure thermal equilibrium during measurements. Room temperature was dependent on centralized building controls, and thus could not be accounted for during experiments. The change in ambient temperature resulted in some discrepancies at very-long acquisition times as some studies were carried out during the day, while others were conducted overnight. These discrepancies are strongly represented in the large standard deviations shown in Figs. 3(a) and 3(c).

2.5 Brillouin spectra acquisition and analysis

Brillouin spectra analysis for all spectrometers was completed using custom batch processing scripts in OriginPro 2017. All spectra were processed using partial-least-squares background subtraction and Lorentz fit methods. Brillouin peak positions (weighted centers) and Brillouin linewidths (FWHM) were determined accordingly. The distance between Stokes and anti-Stokes peaks corresponds to twice the Brillouin shift, so by measuring spectral peak locations we can extrapolate the magnitude of the Brillouin shifts with high accuracy and precision. This analysis allows for a direct look at the performance of each spectrometer against acquisition time, with a focus on accuracy and precision of measurements and spectral resolution.

Though we applied the same background subtraction and Lorentz fit to all spectra, we could not use the same batch processing script for spectra acquired across all three spectrometers. The TFPI spectra contain only three peaks and all detector-pixels are defined with set frequency spacing, making analysis straightforward. The VIPA-based spectra are more complex, composed of multiple non-linearly spaced projections from VIPA to detector. To account for the dispersive nature of the VIPAs and nonlinear spacing of projected Brillouin peaks, we applied a scaling algorithm to normalize the Brillouin shifts across FSR iterations and accurately fit peaks to their respective frequency values [18]. The algorithm follows a heuristic polynomial fit method and uses locations of either the Stokes or anti-Stokes Brillouin peaks (defined by the first, third, fifth, and seventh peak locations by peak finding methods and identified as stokes or anti-stokes by the user) as well as the VIPA FSR to generate a scaling factor - the separation of each Stokes or anti-Stokes peak iteration is assumed to match that of the VIPA FSR. The scaling factor and fit provide the respective frequencies of Brillouin shifts at each position across the detector. Spectra and their analysis are discussed further in the results section of this report.

Optics EXPRESS

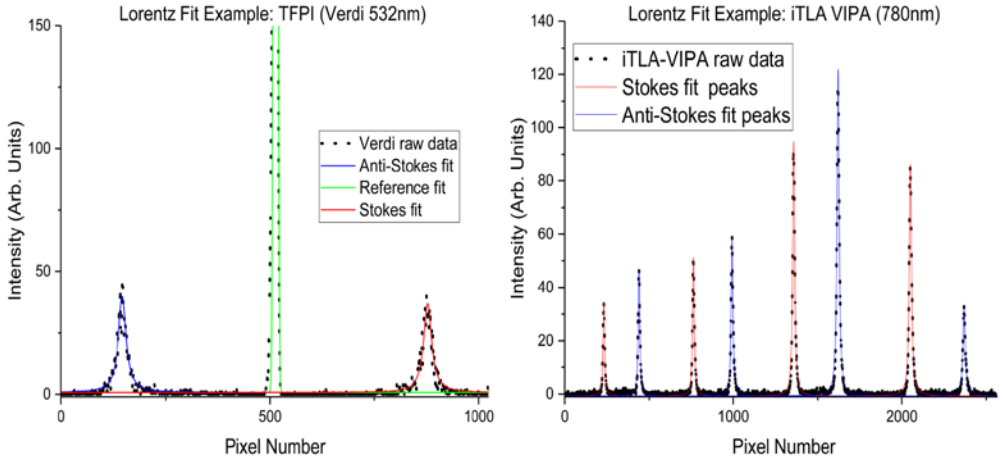

Fig. 2. Raw spectra and the Lorentzian fit examples for TFPI spectra – left, and VIPA spectra – right. Acquisition times for these examples are at 0.512 s and 0.1 s, respectively. The x-axis is provided as pixel number, as this is a spectrum from raw data, and not post-fit analysis.

We repeated each data acquisition cycles 50 times per acquisition time ranging from 0.01 to 1 and 100 s for the 780 nm VIPA-systems and from 0.512 to 102.4 s for the 532 nm TFPI and VIPA systems. The average Brillouin shift and average Brillouin linewidth measurements were then determined for each data acquisition set.

3. Experimental results and discussion

We analyzed Brillouin spectra acquired by three modern Brillouin spectrometers, using the same analysis methods across all data sets to eliminate extra variables between system types. Results of spectra analysis is presented and discussed below. While the purpose of this report is not intended to provide comparative analysis, specific Brillouin shift and Brillouin linewidth (FWHM) measurements are provided in the discussion of each system. The values provided are specific to 0.5 s acquisition time for the 780 nm VIPA-based spectrometer and 0.512 s for the 532 nm TFPI and 532 nm VIPA-based spectrometer. These specific values are provided to give a quantifiable look at the performance of each spectrometer at a specific acquisition time, i.e. the fastest acquisition time that we could achieve with the scanning TFPI and the 532 nm VIPA-based spectrometer at very low power. We determined the optimal acquisition time for each system as the fastest time at which the systems could achieve either the best spectral resolution, or the fastest speed that the system could acquire data while remaining within range of the desired spectral resolution (< 10 MHz).

3.1 Tandem 6-pass Fabry-Perot interferometer

The 6-pass scanning TFPI system recorded a reference beam along with the Brillouin spectra. This reference beam allows for system stabilization during signal acquisition and provides a clear indication of where the known Rayleigh line frequency is. The results of spectra analysis for the TFPI system are presented alongside the spectra analysis from the VIPA-based systems in Figs. 3(a) and 3(b). The spectra acquired using 532 nm incident wavelength are combined into a single graph to allow for a direct look at their performance. Likewise, since two laser sources were used for the TFPI and 780 nm VIPA-based spectrometers, plots from the same system with different lasers are set in overlay, for direct comparison.

The first data set for this investigation was acquired with the TFPI system and Torus 532 laser. Power measured at the sample was approximately 30mW. The averaged Brillouin line shift for acetone was measured as 5.94 ± 0.04 GHz at 0.512 s acquisition time. The averaged Brillouin linewidth was measured to be 678 ± 35 MHz. These measurements are in agreement with the expected value of 5.936 GHz [26]. The TFPI-based spectrometer was set with the mirror spacing corresponding to a FSR = 50 GHz and an inter-channel resolution of 91.7

Optics EXPRESS

MHz for each scan. This mirror spacing gives poor spectral resolution and what appears to be very high precision in measurements. We repeatedly measured peak positions to be in the same position across multiple or even all scan iterations. However, what appears to be an exceptionally low standard deviation in measurements is simply the result of the poor spectral resolution. With this specific mirror spacing, any variance in peak position below ~180 MHz (± 90 MHz) is essentially undetectable.

The issue of poor spectral resolution is easily addressed, however, as a major benefit of TFPI systems is that the mirror spacings for cavities are tunable, and thus can be adjusted to improve FSR and spectral resolution. The tradeoff here is that the signal acquisition time must increase to maintain accuracy. Analysis suggests that the optimal acquisition time for this system with these settings is between 6 and 8 s. Count rates at the Brillouin peak were found to be 2.44 counts/s per mW of incident optical power. Clearly, the low spectral resolution along with less than ideal laser performance was cause for alarm. Therefore, a new SLM laser source (Verdi G2, Coherent Inc.) was used to replicate the experiment with the TFPI mirrors tuned to a more appropriate scan range with FSR = 16.57 GHz and inter-channel resolution of 16.18 MHz. While the original laser source itself may not have been performing well during this experiment, we acknowledge that the primary source for poor spectral resolution was the tuning of the TFPI mirrors, and less-so the performance of the original laser.

Power recorded at the sample with the new SLM laser was approximately 29 mW. The averaged Brillouin line shift for acetone was measured to be 5.92 ± 0.007 GHz at 0.512 s acquisition time. The averaged Brillouin linewidth was measured to be 394 ± 29 MHz. Optimal acquisition time was determined to be between 2 and 3 s. This is a significant improvement over the previous results, indicating a severe dependence on the light source stability and laser line width, as well as the finesse and FSR of the TFPI cavities. While these dependencies are well known, this procedure allowed us to diagnose and significantly improve our TFPI system and to further assess the limits of our spectrometer design with less emphases on individual component limitations.

3.2 VIPA-Based spectrometer at 780 nm with ^{85}Rb absorption cell

The first VIPA-based spectrometer, designed around excitation wavelength of 780 nm, was also tested with two laser sources (ECDL and iTLA). With the ECDL laser source, the averaged Brillouin shift for acetone was measured as 4.09 ± 0.003 GHz. The Brillouin linewidth was measured to be 692 ± 5 MHz. These measurements are in agreement to within 1% of the expected value of 4.039 GHz as calculated from the average index of refraction and speed of sound in acetone [27,28]. Laser power at the sample was approximately 28mW. Photon count-energy ratio of the ECDL VIPA-based setup was found to be 10.38 counts/s per mW of incident optical power at the reported 0.5 s acquisition time. The optimal acquisition time for the 780 nm VIPA-based system with ECDL source was between 70 and 100 ms. Spectra were obtainable at faster acquisition times; however, the SNR began to degrade significantly from roughly 10dB at 100ms to almost 1dB at 20ms. Acquisition times longer than 100 ms do not provide for improved measurements, but rather increase the risk of external and environmental disruptions and laser drift. These undesired effects are demonstrated by the remarkable increase in standard deviation of Brillouin linewidth measurements shown in Fig. 3(d) for the two longest acquisition times with the ECDL. We determined that the drastic increase in standard deviation was likely due to instability in the laser source; i.e. the result of drift in laser wavelength, or the result of a laser mode hop.

We installed the iTLA source for the 780 nm VIPA-based system to overcome the instability experienced with the ECDL source and to eliminate the extra materials and electronic locking system needed to control the piezo device. Essentially, the iTLA laser was installed to simplify the system and provide a more reliable and more narrow-band excitation source. With the iTLA source, we repeated the experiment for acquisition times up to 1 s. The results of analysis are presented in Figs. 3(c) and 3(d) in overlay with the previous ECDL results allowing for a quick look and direct comparison. Longer acquisition times were

Optics EXPRESS

omitted, since previous experiments and analysis had proven that longer acquisition times were of no benefit and the overall goal was to evaluate the spectrometer performance at faster acquisition times.

With the iTLA source at 0.5 s acquisition time, the averaged Brillouin shift for acetone was measured as 4.10 ± 0.003 GHz. The Brillouin linewidth was measured to be 511 ± 5 MHz. These results are within ~1.5% the expected value of 4.039 GHz. Optimal acquisition time for the 780 nm VIPA-based system with iTLA source was between 20 and 50 ms, faster than any previous reports for single-point acquisition for spontaneous Brillouin. In fact, longer acquisition times than this did not provide for any improvements in accuracy or spectral resolution. The iTLA technology is based on lasers used in the Telecom industry, modified by the manufacturer to meet the stringent requirements of high SNR applications like those in a spectroscopy laboratory setting. As with the TFPI results, we see a strong dependence on laser source when looking at the linewidth measurements between the ECDL and iTLA lasers. This iTLA laser has excellent stability and more narrow-band output than the ECDL laser that was originally used, and thus provides for much better results.

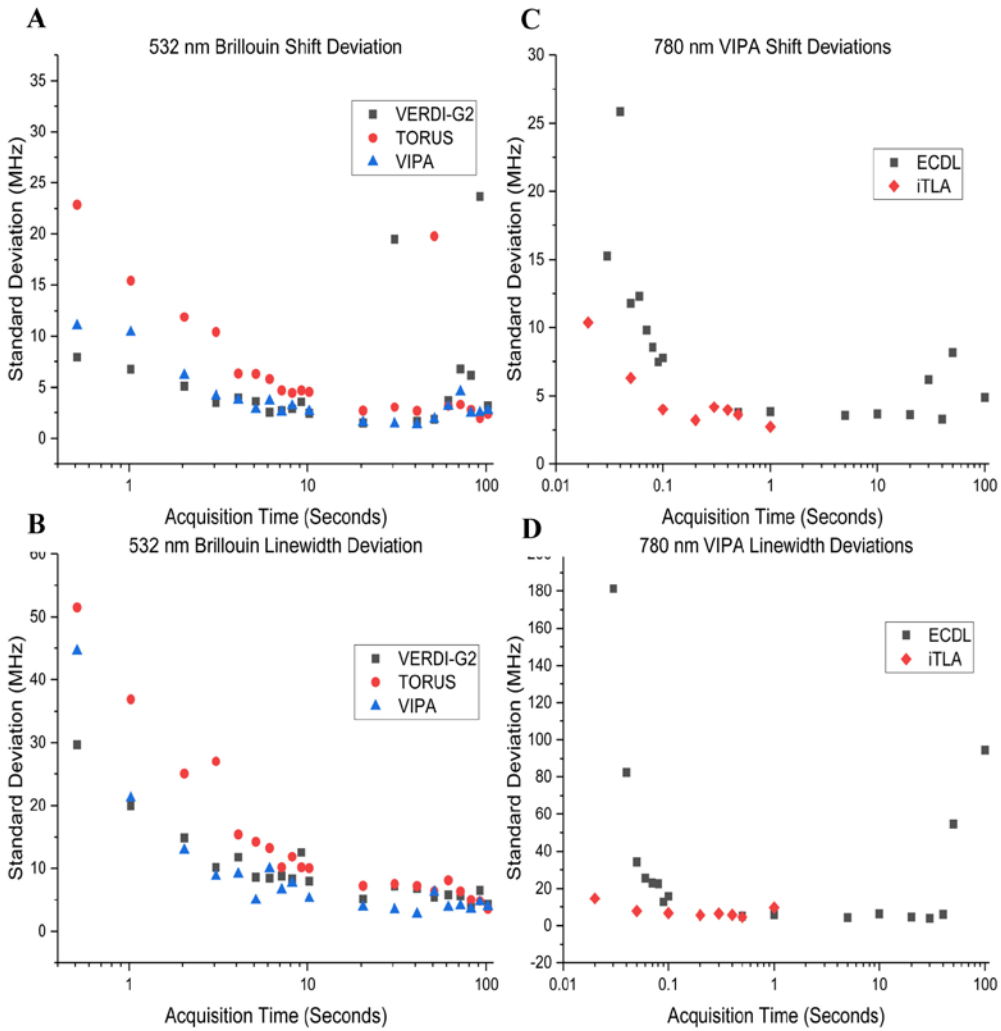

Fig. 3. Standard deviations for Brillouin shifts (A) and linewidths (B) from 532nm TFPI – with black squares (Torus) and red circles (Verdi) for the two laser sources, blue triangles for VIPA-based system; 780 nm VIPA-based Brillouin shifts (C) and linewidths (D) – with black squares for original ECDL laser and red diamonds for new iTLA-based laser setup.

Optics EXPRESS

3.3 VIPA-Based spectrometer at 532nm with Iodine absorption cell

The second VIPA-based spectrometer matched the 532 nm excitation wavelength of the TFPI spectrometer, and analysis results are shown in overlay with TFPI results in Figs. 3(a) and 3(b). With the 532 nm VIPA-based spectrometer, the averaged Brillouin shift for acetone was measured as 6.05 ± 0.032 GHz, with a linewidth of 905 ± 44 MHz at 0.512 s acquisition time. These results are within 2% of the expected value (again, 5.936 GHz). As shown in Fig. 3(b), the Brillouin linewidth measurements from this system are much greater than that of the TFPI system. The difference in linewidth is in-part due to the high NA of the microscope objective used, and the properties of the VIPA for this spectrometer. Likewise, a recent report and our own analysis has pointed to a potential for further optimization of the cylindrical lens leading to the VIPA input, and the position and angle of the VIPA to the spherical lens and detector to improve linewidth measurements and spectral resolution [1,11]. Optimal acquisition time for this spectrometer was determined to be between 1 and 2 s. It is possible for this spectrometer to achieve results equal to and even greater than this at faster acquisition times. However, since incident laser power was set very low to allow for detection at longer acquisition times, spectra from acquisition times faster than this were sub-optimal and noisy with too low a SNR to analyze effectively.

4. Summary and Discussion

In summary, we have assessed the performance of three modern Brillouin spectrometers of two different designs and excitation wavelengths, and report the fastest spontaneous Brillouin measurements to date. The spectrometers evaluated were a conventional scanning 6-pass TFPI system at 532 nm and two custom-built VIPA-based spectrometers with atomic absorption-based notch filters at 532 nm and 780 nm respectively. Brillouin spectra were acquired from acetone, a common standard for Brillouin measurements often used as a calibration sample. Throughout the investigation, we were successful in using our analysis to evaluate and diagnose potential issues with our spectrometers. We clearly demonstrated the dependence of measurement reliability on excitation source quality, a critical issue with Brillouin spectrometer design.

Our analysis showed the scanning 6-pass TFPI system (with the new SLM laser) had its most reliable measurements, with lowest standard deviation in Brillouin shift, linewidth as well as greatest accuracy, at acquisition times between 2 and 3 s. While this is significantly faster than the acquisition times of older systems, total scan times still broach on several minutes for a complete sequence of 50 iterations. However, a primary strength of this design is that spectral resolution of a TFPI is determined by an inverse relationship with finesse ($1/\boldsymbol{F}$) of the Fabry-Perot cavity, and thus can be fine-tuned to meet the needs of the sample and individual situations.

With the 532 nm VIPA-based spectrometer, we maintained a significantly lower laser power at the sample ~0.8 mW, compared to the other spectrometers. Though lower than desired, this power level was maintained for all spectra acquisition time to maintain uniformity throughout the experiment. As stated previously, this power level was chosen to avoid detector saturation at long acquisition times (greater than 10 s). This low laser power provided for poor resolution and low signal-noise ratio (SNR) at fast acquisition times (less than 0.5 s). Since both 532 nm and 780 nm spectrometers follow the same design and quantities of interest in Brillouin measurements are often sound velocity and stiffness tensor elements, our primary focus for discussing the VIPA-based spectrometer performance is that of the 780 nm spectrometer. This is due in part to the low incident power of the 532 nm system, but also because sound velocity scales directly with wavelength, thus a small uncertainty in frequency shift measurements at 780 nm would be more significant than at 532 nm.

The most reliable measurements for our 780 nm VIPA-based design were determined to be at acquisition times between 20 and 50 ms. Today, the fastest single-point acquisition times that have been reported for spontaneous Brillouin measurements were at 50 ms, since

Optics EXPRESS

below 100 ms, SNR is often too low for reliable measurements. Here, we report measurements as fast as 20 ms acquisition time, more than two times faster than the fastest times previously reported [14]. Since VIPAs are made of a single prism of fixed dimensions, a potential approach to achieving greater spectral resolution, would be to design an interchangeable stage with multiple VIPAs of different FSR, chosen based on the needs of each experimental. The closer the FSR is to the expected Brillouin shift, the greater accuracy and resolution one can expect.

Laser stability and the quality of optical components are the primary factors in determining the overall quality, accuracy, and spectral resolution of Brillouin spectrometer measurements, and spectrometer design has the most significant impact on acquisition speed. The accuracy of Brillouin measurements is influenced by spectra signal-to-noise ratio, which is determined by input laser power, scattering efficiency (wavelength dependent), throughput of the spectrometer, sensitivity of the detector, quality of optical components, and a variety of other factors. Basically, since modern custom-built spectrometers (such as Brillouin spectrometers in research laboratories) are designed around a wide range of available laser sources and optical components this means that each spectrometer should have its own optimal acquisition time "sweet-spot" for achieving high accuracy and spectral resolution [1,11,29]. External conditions such as environment temperatures and mechanical vibrations can also play a role in determining how well spectrometers perform, but these conditions are not critical to spectrometer design and can be accounted for by sample isolation or through corrections in data analysis.

Finally, we note that acetone - the sample utilized in this experiment, is often used as a calibration sample for Brillouin spectroscopy and does not present the same challenges that more turbid or opaque samples may present. In this regard, the more conventional TFPI systems have historically been more reliable and accurate for Brillouin spectroscopy measurements. Recent developments in VIPA-based spectroscopy related to increased elastic extinction ratios and background subtraction have led to significant advances [2,17,30], and future studies relating the performance of such systems with turbid and highly-scattering samples may provide further insight along with the data presented in this study.

By evaluating the performance of our spectrometers, we were successful in identifying and correcting for specific issues and achieved improvements in overall performance, even reporting the fastest signal acquisition times to date for a single-point acquisition of Brillouin spectra. We hope to use the information gathered from this experiment to guide future designs and development of Brillouin spectrometers and hopefully provide direction for overcoming limitations inherent to each spectrometer design.

Funding

National Science Foundation (NSF) (DBI-1455671, DBI-1532188, ECCS-1509268); US Department of Defense (DOD) (FA9550-15-1-0517, N00014-16-1-2578), Cancer Prevention Research Institute of Texas (CPRIT) (RP160834), Nazarbayev University (SST2015014) and the state-targeted programs Ministry of Education and Science of the Republic of Kazakhstan (BR05236524 and BR05236454).